International Journal of Science and Research (IJSR)
ISSN: 2319-7064
Impact Factor 2024: 7.101

Cytotoxicity Evaluation of ZnO NPs Based Resin Nanocomposite Using MTT Assay: A Sustainable Approach for Restorative Dentistry

Shravani Wadekar[1], Manish Hate[2], Ramesh Chaughule[3]

[1]Research Student, Ramnarain Ruia Autonomous College, L. N. Road, Matunga (east), Mumbai- 400019, India
Email: *shravaniwadekar996[at]gmail.com*

[2]Head of the Chemistry Department, Ramnarain Ruia Autonomous College, L. N. Road, Matunga (East), Mumbai-400019, India.
Email: *manishS[at]gmail.com*

[3]Ex. Tata Institute of Fundamental Research, Mumbai, India Adjunct Professor, Ramnarain Ruia Autonomous College, Mumbai, India.
Email: *rsctifr[at]yahoo.com*

Abstract: ***Oral caries affects individuals across all age groups and, if untreated, can lead to tooth loss, infections, and systemic complications, emphasizing the need for timely dental care and proper oral hygiene. As a result, there is a growing demand for effective, durable, and sustainable dental solutions. Nanotechnology, with its exceptional physical, chemical, and mechanical properties, shows immense promise in dentistry. This study involved the green synthesis of zinc oxide nanoparticles (ZnO NPs) using plant extracts, which were incorporated into resin matrices to create resin bio-nanocomposites. Traditional Bis-GMA resin was replaced with GMA and UDMA polymers, cured using a light-curing unit. The resulting composites were analysed using FTIR-ATR and Raman spectroscopy to explore bonding interactions between polymers and nanoparticles. Mechanical properties were assessed through tensile, flexural, and compressive strength tests. Cytotoxicity was evaluated using a dose-dependent MTT assay on NIH-3T3 fibroblast cell lines. ZnO NPs-based composites were compared with TiO_2 NPs, their combination, and commercial Spectrum samples. Results revealed that ZnO NPs composites had superior mechanical performance, particularly at higher concentrations, and lower cytotoxicity at reduced doses. These findings support their potential as functional and aesthetically suitable materials for restorative dentistry applications.***

Keywords: ZnO NPs, Resin nanocomposites, MTT assay, NIH-3T3 Fibroblast cell-line, Cytotoxicity.

1. Introduction

The healthcare sector continuously seeks to enhance medical services through technological innovations globally [1]. Nanotechnology has emerged as a crucial component of healthcare, offering an enhanced perspective with practical applications in medicine [1]. A significant revolution in science has elevated humanity to a new domain known as nanotechnology. Nanomedicine is a comprehensive domain of research and technology focused on illness treatment, diagnosis, human health, medical enhancement, and nanoscale technologies [1]. Nano-dentistry is an emerging discipline that employs nanomaterials, nanorobots, and nanotechnology for the diagnosis, treatment, and prevention of dental caries [2]. The primary emphasis is on the targeted delivery of medicinal and diagnostic agents [1]. Nanotechnology relies on the structural properties of a material and is contingent upon the substance's dimensions for optimal functionality [1], [3].

Researchers are attempting to identify a composite material that can replicate dentinal tissue and restore the original dental aesthetics, which is regarded as a problem. The integration of nanoparticles with a resin matrix is a barrier in the progression of dental nanomaterials. The objective is to create a robust, attractive, and biocompatible product that facilitates ease of handling for both physicians and patients [1]. Dental chemistry has been utilized in several dental procedures, including cavity restoration, tooth whitening, and orthodontic therapy. Addressing oral germs is crucial when considering restorative materials; therefore, nanomaterials such as gold, silver, and titanium dioxide nanoparticles are used to enhance their antibacterial characteristics [1]. Metallic and metal oxide nanoparticles are utilized as fillers in dental composite materials. The primary objective of incorporating dental filler is to inhibit the proliferation of pathogens, particularly *Streptococcus mutans*, which is typically located between the enamel and tooth restorations [3]. Nanomaterials possess the ability to address diverse dental issues owing to their bioavailability, effectiveness, and enhanced dose reduction [1]. Soon, nanomaterials, with their sophisticated techniques and enhanced capabilities, will influence several applications.

This study employed the aqueous extract of *Cassia fistula* leaves to synthesize Zinc oxide nanoparticles (ZnO NPs) via an environmentally benign method that obviates the necessity for hazardous reagents and energy-intensive procedures, as previously documented [9]. The biosynthesized ZnO NPs were subsequently incorporated into a resin nanocomposite matrix consisting of GMA, UDMA, and APTES, along with the photo-initiator CQ, to create an innovative dental restorative material. The ZnO NP-based resin nanocomposite demonstrates augmented antibacterial efficacy, enhanced mechanical stability, and superior adhesion, rendering it a viable and sustainable option for oral healthcare. By integrating biocompatibility with environmentally conscious synthesis and advanced functional performance, this material signifies a promising advancement toward comprehensive, cost-effective dental care solutions that fulfil both clinical and environmental objectives.

2. Literature Survey

In the past decade, resin nanocomposites have been utilized in dentistry for both anterior and posterior tooth restorations. Historically, amalgam-based materials were utilized, but their use has been reduced due to aesthetic and toxicological concerns [4]. The word "composite" refers to a material composed of multiple components. This definition indicates that resin composite mostly comprises glass ionomers, ceramics, fillers, and other materials incorporated inside it [5]. Cement and glass ionomers are commonly utilized as restorative materials for the treatment of secondary caries [5]. It functions as a sealant, releases fluoride, and aids in the remineralization process [5]. The term dental composite restorative resin is an alternative to tooth-coloured materials. This is the primary advantage over traditional dental amalgam. However, it possesses several disadvantages, including brittleness, reduced durability, limited flexibility, inadequate tensile strength, and inferior aesthetics, which exclude its usage by dentists [5]. This obstacle can be surmounted by employing resin-based nanofillers, which exhibit enhanced mechanical, physical, and chemical capabilities [5].

Resin serves as the primary component of the matrix and is selected for its capacity to polymerize. The polymerization process commences under the influence of light, heat, or other particular conditions [5], [6]. Additionally, certain processes occur in photocatalytic conditions. This process is crucial as it converts monomers (small molecules) into polymers (long chains of monomers). The composite consists of two phases: the organic phase (matrix) and the inorganic phase (filler), which is mixed with the coupling reagent [5]. The last phase is initiated by the addition of a photo-initiator to commence the polymerization process. The components within the matrix may not engage in the polymerization process until they undergo curing. The curing of the material is crucial; otherwise, exposure of the surface layer to air or moisture results in incomplete polymerization. The application of a light-curing device alters the properties of the material, particularly the resin matrix, which may undergo condensation, polymerization, or addition reactions [5]. Such reactions resulted in the formation of stiff polymer molecules. Polymethylmethacrylate (PMMA) exhibits enhanced mechanical strength when integrated with a resin nanocomposite. Dimethacrylates are extensively utilized due to their superior mechanical strength, ease of handling, fast polymerization, and capacity to connect with tooth enamel. Consequently, dimethacrylates such as bisphenol A glycidyl methacrylate (Bis-GMA), triethylene glycol dimethacrylate (TEGDMA), and urethane dimethacrylate (UDMA) are commonly employed [5]. Bis-GMA serves as the primary component of the matrix, exhibiting high viscosity, excellent surface hardness, and superior heat conductivity; hence, it extends its shelf life. This sticky resin is diluted with 3-aminopropyl triethoxysilane (APTES) to enhance handling efficiency. UDMA exhibits relatively low viscosity, enhancing flexibility and wear resistance [5]. This combination also possesses the capability to solubilize the substance in a specific solvent.

Without inorganic fillers, this combination would exhibit low mechanical strength; hence, the incorporation of inorganic fillers is necessary [5]. A diverse array of nanofillers is utilized, including silica (crystalline quartz), carbon nanotubes, nano zinc, nano alumina, zirconia, nano hydroxyapatite, and titanium dioxide nanoparticles (TiO_2 NPs) [5]. In addition to nanofillers, photo-initiators are incorporated, which are responsible for photoreactions and the generation of reactive oxygen species. Camphorquinone (CQ), a blue light photo-initiator, is frequently utilized in dental resin compositions. Various resin materials necessitate distinct light-curing techniques [5]. The selection of nanoparticles is predicated on their physical attributes, particularly tensile strength, flexural strength, compressive strength, wear resistance, polymerization shrinkage, microhardness, and aesthetic appearance (including patient concerns).

The integration of metal and metal oxide nanoparticles into resin-based composites has demonstrated significant potential in enhancing antibacterial efficacy, mechanical strength, and aesthetic qualities. ZnO NPs are distinguished among different nanoparticles for their superior antibacterial, antifungal, and physicochemical capabilities [4]. ZnO NPs are highly effective in compromising bacterial cell membranes, reducing biofilm formation, preventing secondary cavities, demonstrating enhanced adhesion qualities, and remaining non-toxic and environmentally friendly [7]. The biosynthesis of ZnO NPs via plant extracts provides an environmentally friendly and sustainable alternative to conventional chemical and physical synthesis techniques [8], [9].

3. Methodology

3.1 Synthesis of ZnO NPs:

ZnO NPs were manufactured using a previously published green synthesis method, wherein the plant extract acted as both the reducing and stabilizing agent, as previously reported [10]. The resultant nanoparticles were characterized using several hyphenated analytical techniques, including ultraviolet-visible spectroscopy (UV-Vis), Fourier transform infrared spectroscopy (FTIR), powder X-ray diffraction (PXRD), field emission scanning electron microscopy (FESEM), high-resolution transmission electron microscopy (HRTEM), and energy dispersive X-ray analysis (EDAX), as demonstrated in prior research [10].

3.2 Synthesis for Resin Nanocomposites:

Resin bio-nanocomposites were synthesized according to the protocol mentioned earlier [11].

3.3 Experimental Setup for Cytotoxicity Testing with NIH3T3 Fibroblast Cell Line:

The mouse embryonic fibroblast cell line NIH-3T3 was procured from the National Center for Cell Line (NCCS), Pune. Cell culture media—DMEM medium supplemented with 10% Fetal Bovine Serum (FBS), MP Biomedicals, Germany.1X Dulbecco's Phosphate Buffered Saline (DPBS), 0.25% Trypsin-EDTA solution, and MTT reagent were all purchased from MP Biomedicals, Germany. Dimethyl Sulfoxide (DMSO), cell culture grade, Merck, Germany. Cell

culture treated T-25 flasks from Biolite, Thermo Fisher Scientific Inc., USA.10 mL serological pipettes and 96-well plates from Nunc, Thermo Fisher Scientific Inc., USA.5mL, 2 mL, and 1.5 mL tubes, Tarsons, India. Class II A2 Biological Safety Cabinet-BSC-1300IIA2-X, Biobase, China. CO_2 Incubator—ZOCR-1150B, Labwit, Australia. Microscope-XDFL series, Sunny Instruments, China. Image analysis software—ImageJ (Fiji) version 1.53j. Microplate reader—BK-EL10A from Biobase, China.

3.4 In-vitro Cytotoxicity Study of Nanoparticles-Based Resin Nanocomposites:

The MTT assay was used to measure cytotoxicity in NIH3T3 fibroblasts. A concentration-percentage cell viability graph was created. The seven samples included six tests and one control. Each concentration was made by dissolving the chemical in DMSO. Each sample was dissolved in 5 mL of 1% w/v solvent at 0.05 g. Boiling the solution in water produced homogeneity. The samples were cooled and stored in airtight, amber-coloured glass containers under cool, dry conditions after dissolution. Table 1 lists sample specifications and arrangements for MTT treatment.

3.5 Procedure for MTT-based Cytotoxicity Assessment:

1) Cells cultivated in T-25 flasks were trypsinized and subsequently transferred into 5 mL centrifuge tubes. The cells were subsequently centrifuged at 300 × g to acquire a cell pellet. The pellet was resuspended in DMEM-High Glucose (DMEM-HG) medium, and the cell concentration was calibrated to ensure that 200 µL of the suspension contained about 10, 000 cells.
2) Each well of a 96-well microtiter plate was inoculated with 200 µL of the cell suspension and incubated at 37°C in a 5% CO_2 environment for 24 hours to facilitate cell adhesion and proliferation. Following the incubation period, the spent medium was aspirated, and 200 µL of different concentrations of the test samples were introduced into the corresponding wells.
3) The dish was incubated once more under identical conditions for an additional 24 hours. Subsequently, the media containing the test sample was discarded, and 200 µL of fresh medium with 10% MTT reagent was introduced to each well, achieving a final MTT concentration of 0.5 mg/mL.
4) The plate was subsequently incubated for 3 hours at 37°C in a 5% CO_2 environment to facilitate formazan crystal production by metabolically active cells. Thereafter, the medium was meticulously extracted without disrupting the crystals, and 100 µL of DMSO was introduced to each well to solubilize the formazan.
5) The plate was delicately agitated with a gyratory shaker to guarantee thorough disintegration. Absorbance was quantified with a microplate reader at 570 nm, with a reference wavelength of 630 nm.
6) Following background and blank removal, the percentage of cell growth inhibition was computed, and the IC_{50} value (the concentration of the test substance necessary to inhibit 50% of cell growth) was ascertained from the dose-response curve for the cell line. The sample details and visuals details are listed in Table1 and Figure 1.

Table 1: Summarizes the test samples details and their corresponding IC_{50} values

Sample details	Cell line	Result
S1 – ZnO NPs Test range– 1.25-30 %v/v Incubation time – 24h	NIH-3T3	IC_{50} = 6.37 %v/v
S2 – TiO_2 NPs Test range– 1.25-30 %v/v Incubation time – 24h	NIH-3T3	IC_{50} = 6.91 %v/v
S3 – ZnO+TiO_2 NPs Test range– 1.25-30 %v/v Incubation time – 24h	NIH-3T3	IC_{50} = 7.13 %v/v
S4 – TiO_2 NPs + Spectrum Test range– 1.25-30 %v/v Incubation time – 24h	NIH-3T3	IC_{50} = 6.32 %v/v
S5 – ZnO NPs + Spectrum Test range– 1.25-30 %v/v Incubation time – 24h	NIH-3T3	IC_{50} = 6.99 %v/v
S6 – ZnO powder + Spectrum Test range– 1.25-30 %v/v Incubation time – 24h	NIH-3T3	IC_{50} = 6.74 %v/v
S7 – Control Test range– 1.25-30 %v/v Incubation time – 24h	NIH-3T3	IC_{50} = 5.05 %v/v

Samples 1 -7 were tested within a concentration range of 1.25 v/v to 30.0 v/v, with a 24-hour incubation period. Their respective IC_{50} values were determined, revealing a varying degree of potency among the samples. This highlights the significance of concentration in achieving effective inhibition. Further analysis will explore the mechanisms underlying the differences in IC_{50} values. Further analysis will focus on the underlying mechanisms responsible for these differences in IC_{50} values.

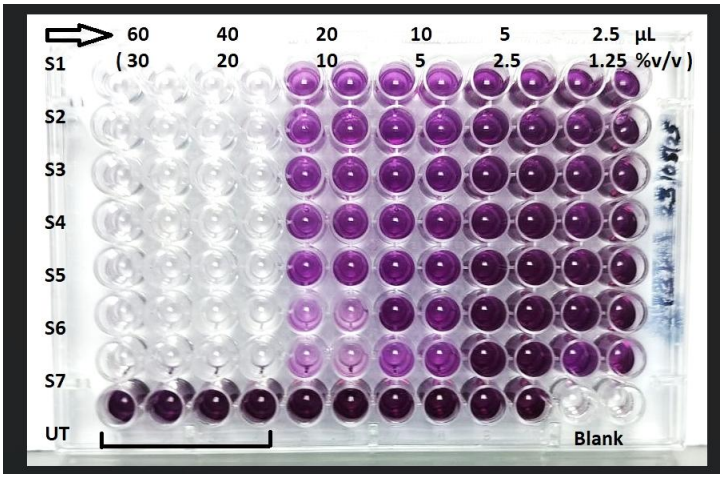

Figure 1: Visual representation of MTT assay cytotoxicity evaluation results of the test samples S1 to S7

4. Results

4.1 Mechanical characterization of resin-based bio-nanocomposites:

The biosynthesis of ZnO NPs and their mechanical properties for ZnO NPs and TiO_2 NPs based resin nanocomposites were evaluated by assessing tensile strength, flexural strength, and compressive strength as reported earlier [9], [10].

4.2 Structural and Morphological Characterization of Resin Nanocomposites

4.2.1 Fourier Transform Infrared Spectroscopy-Attenuated Total Reflectance (FTIR-ATR):

A PerkinElmer Spectrum Two spectrometer with an attenuated total reflectance (ATR) accessory were used to obtain Fourier-transform infrared (FTIR) spectra on resin nanocomposites to predict functional groups, especially due to ZnO NPs and the polymer matrix (GMA, UDMA, APTES, PVA, and CQ). Spectra were collected at a resolution of 4 cm^{-1} from 4000 to 400 cm^{-1}, with an average of 32 scans per sample. Spectral interpretation of peaks from the PerkinElmer Spectrum 10 program was performed. Figures 2, Figure 3, and Figure 4 show nanoparticle presence and stability in the polymer matrix at three concentrations.

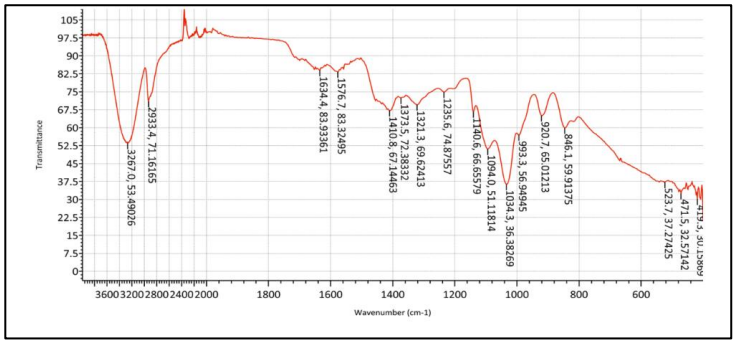

Figure 2: FTIR-ATR analysis of sample containing 0.05g ZnO NPs in resin matrix

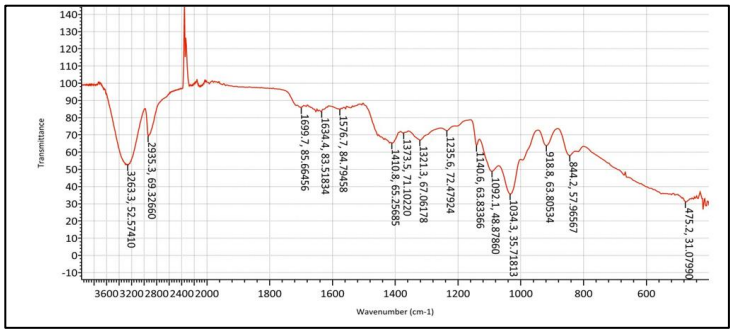

Figure 3: FTIR-ATR analysis of sample containing 0.05 g TiO_2 NPs in resin matrix

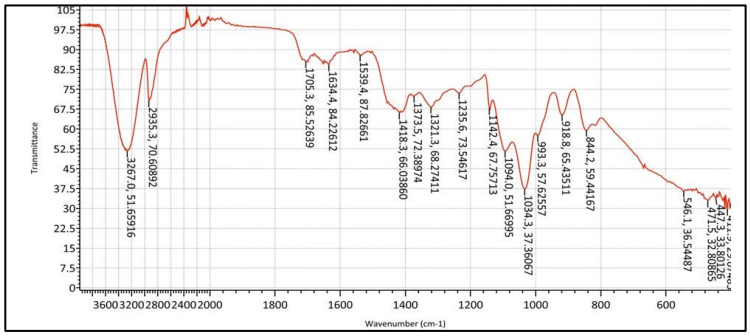

Figure 4: FTIR-ATR analysis of a sample containing 0.1 g TiO_2 NPs and 0.1g ZnO NPs in resin matrix

4.2.2 Raman Spectroscopy

A HORIBA LabRAM HR Evolution Raman spectrometer with a 532 nm laser excitation source and 1800 lines/mm grating was used for RAMAN spectroscopy. Measurements were taken from 0 to 4000 cm^{-1} using a 20× VIS objective lens, 200 µm slit width, and 500 µm hole diameter. Spectra were acquired with five accumulations and a three-second scan. To improve spectral precision, ICS correction was activated. The RAMAN spectra for 0.05g ZnO NPs, 0.05g TiO2 NPs, and 0.1 g TiO2 NPs and ZnO NPs are depicted in Figure 5, Figure 6 and Figure 7 respectively.

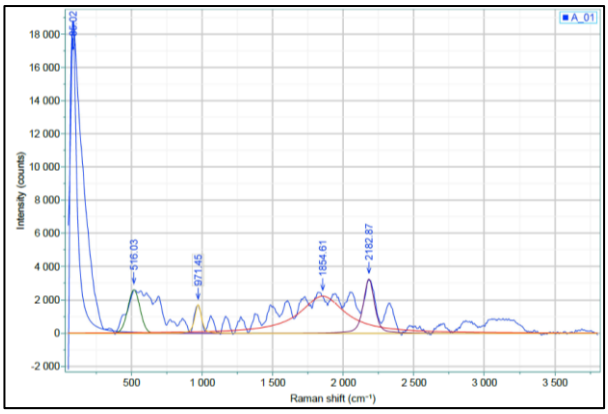

Figure 5: Raman spectroscopic analysis of resin nanocomposite containing 0.05 g ZnO NPs

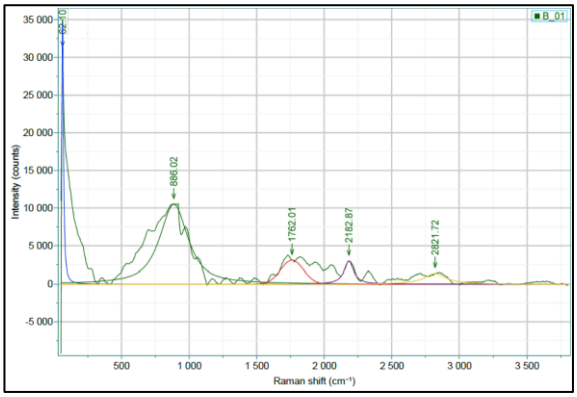

Figure 6: Raman spectroscopic analysis of resin nanocomposite containing 0.05 g TiO_2 NPs

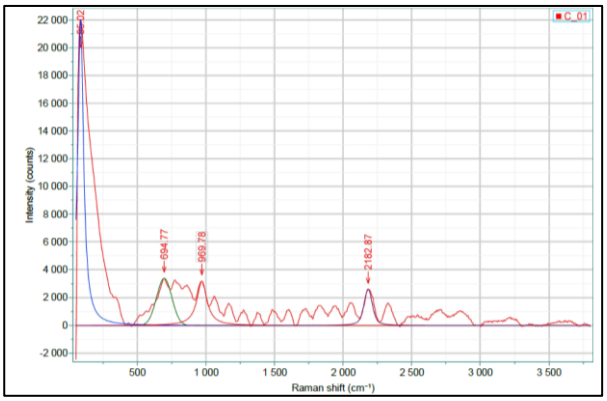

Figure 7: Raman spectroscopic analysis of resin nanocomposite containing 0.1 g ZnO NPs and 0.1 g TiO2 NPs

4.2.3 Field Emission Scanning Electron Microscopy (FESEM):

The FESEM analysis clarifies the surface morphology of the resin matrix containing nanoparticles, revealing either a uniform dispersion or aggregation of the particles, as depicted in Figures 8, Figure 9 and Figure 10.

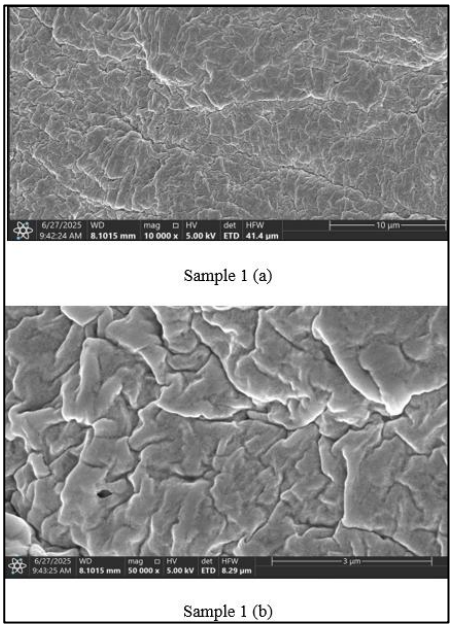

Figure 8: FESEM analysis of sample containing ZnO NPs with resin matrix

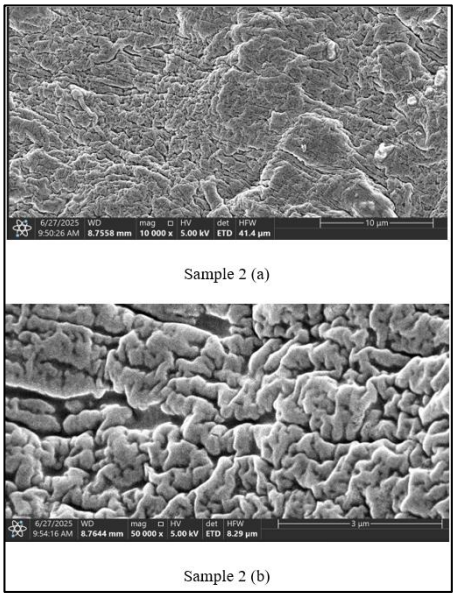

Figure 9: FESEM analysis of sample containing TiO_2 NPs with resin matrix

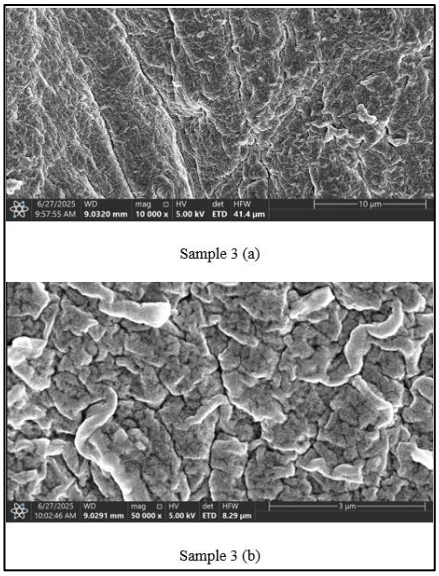

Figure 10: FESEM analysis of sample containing ZnO NPs and TiO_2 NPs with resin matrix

4.2.4. MTT Assay Results: Cell Viability Analysis against Concentration of Sample in %v/v.

MTT assay data consisting of 2.5 µL to 60 µL and the corresponding % viability were calculated (Table 2 to Table 8). The results indicate a clear correlation between the volume of the reagent used and cell viability. The MTT assay was employed to assess cytotoxicity in the NIH3T3 fibroblast cell line. A graph was constructed depicting percentage cell viability in relation to concentration. Six test samples were assessed in addition to a control, resulting in a total of seven samples. Each sample concentration was formulated by dissolving the substance in dimethyl sulfoxide (DMSO). Exactly 0.05 g of each sample was measured and dissolved in 5 mL of the solvent (1% w/v). The solution was boiled in a water bath until homogeneity was achieved. After dissolution, the samples were permitted to cool and were then stored in airtight, amber-coloured glass containers in cool, dry conditions for future use. The specifications and arrangement of the samples for MTT treatment are mentioned in Table 1.

Table 2: Represents percentage cell viability of ZnO NPs based resin nanocomposite (Sample 1) against NIH-3T3 fibroblast cell line

			Concentration (in %v/v)					
	Blank	Untreated	1.25	2.5	5	10	20	30
Volume µL			2.5	5	10	20	40	60
Reading 1	0.08	1.998	1.741	1.774	1.159	0.89	0.097	0.106
Reading 2	0.077	1.884	1.825	1.739	1.152	1.011	0.116	0.106
Mean OD	0.079	1.941	1.783	1.757	1.156	0.951	0.107	0.106
Mean OD-Mean Blank		1.8625	1.7045	1.6780	1.0770	0.8720	0.0280	0.0275
Standard deviation		0.0806	0.0594	0.0247	0.0049	0.0856	0.0134	0.0000
Standard error		0.0570	0.0420	0.0175	0.0035	0.0605	0.0095	0.0000
% Standard error		3.0604	2.2550	0.9396	0.1879	3.2483	0.5101	0.0000
% Viability		100	91.52	90.09	57.83	46.82	1.50	1.48

Table 3: Represents percentage cell viability of TiO_2 NPs based resin nanocomposite (Sample 2) against NIH-3T3 fibroblast cell line

			Concentration (in %v/v)					
	Blank	Untreated	1.25	2.5	5	10	20	30
Volume µL			2.5	5	10	20	40	60
Reading 1	0.08	1.998	1.719	1.834	1.333	0.937	0.107	0.099
Reading 2	0.077	1.884	1.88	1.839	1.34	0.978	0.127	0.105
Mean OD	0.079	1.941	1.800	1.837	1.337	0.958	0.117	0.102
Mean OD-Mean Blank		1.8625	1.7210	1.7580	1.2580	0.8790	0.0385	0.0235
Standard deviation		0.0806	0.1138	0.0035	0.0049	0.0290	0.0141	0.0042
Standard error		0.0570	0.0805	0.0025	0.0035	0.0205	0.0100	0.0030
% Standard error		3.0604	4.3221	0.1342	0.1879	1.1007	0.5369	0.1611
% Viability		100	92.40	94.39	67.54	47.19	2.07	1.26

Table 4: Represents percentage cell viability of ZnO NPs + TiO_2 NPs based resin nanocomposite (Sample 3) against NIH-3T3 fibroblast cell line

			Concentration (in %v/v)					
	Blank	Untreated	1.25	2.5	5	10	20	30
Volume µL			2.5	5	10	20	40	60
Reading 1	0.08	1.998	1.75	1.879	1.378	0.939	0.091	0.101
Reading 2	0.077	1.884	1.846	1.969	1.389	1.00	0.105	0.101
Mean OD	0.079	1.941	1.798	1.924	1.384	0.970	0.098	0.101
Mean OD-Mean Blank		1.8625	1.7195	1.8455	1.3050	0.8910	0.0195	0.0225
Standard deviation		0.0806	0.0679	0.0636	0.0078	0.0431	0.0099	0.0000
Standard error		0.0570	0.0480	0.0450	0.0055	0.0305	0.0070	0.0000
% Standard error		3.0604	2.5772	2.4161	0.2953	1.6376	0.3758	0.0000
% Viability		100	92.32	99.09	70.07	47.84	1.05	1.21

Table 5: Represents percentage cell viability of TiO_2 NPs with commercial resin (Sample 4) against NIH-3T3 fibroblast cell line

			Concentration (in %v/v)					
	Blank	Untreated	1.25	2.5	5	10	20	30
Volume µL			2.5	5	10	20	40	60
Reading 1	0.08	1.998	1.887	1.666	1.124	0.761	0.112	0.12
Reading 2	0.077	1.884	1.883	1.801	1.137	0.928	0.117	0.108
Mean OD	0.079	1.941	1.885	1.734	1.131	0.845	0.115	0.114
Mean OD-Mean Blank		1.8625	1.8065	1.6550	1.0520	0.7660	0.0360	0.0355
Standard deviation		0.0806	0.0028	0.0955	0.0092	0.1181	0.0035	0.0085
Standard error		0.0570	0.0020	0.0675	0.0065	0.0835	0.0025	0.0060
% Standard error		3.0604	0.1074	3.6242	0.3490	4.4832	0.1342	0.3221
% Viability		100	96.99	88.86	56.48	41.13	1.93	1.91

Table 6: Represents percentage cell viability of ZnO NPs with commercial resin (Sample 5) against NIH-3T3 fibroblast cell line

			Concentration (in %v/v)					
	Blank	Untreated	1.25	2.5	5	10	20	30
Volume µL			2.5	5	10	20	40	60
Reading 1	0.08	1.998	1.853	1.85	1.269	0.878	0.103	0.101
Reading 2	0.077	1.884	1.892	1.965	1.293	0.991	0.101	0.099
Mean OD	0.079	1.941	1.873	1.908	1.281	0.935	0.102	0.100
Mean OD-Mean Blank		1.8625	1.7940	1.8290	1.2025	0.8560	0.0235	0.0215
Standard deviation		0.0806	0.0276	0.0813	0.0170	0.0799	0.0014	0.0014
Standard error		0.0570	0.0195	0.0575	0.0120	0.0565	0.0010	0.0010
% Standard error		3.0604	1.0470	3.0872	0.6443	3.0336	0.0537	0.0537
% Viability		100	96.32	98.20	64.56	45.96	1.26	1.15

Table 7: Represents percentage cell viability of commercial ZnO powder with commercial resin (Sample 6) against NIH-3T3 fibroblast cell line

			Concentration (in %v/v)					
	Blank	Untreated	1.25	2.5	5	10	20	30
Volume µL			2.5	5	10	20	40	60
Reading 1	0.08	1.998	1.855	1.929	1.475	0.499	0.289	0.129
Reading 2	0.077	1.884	1.862	1.85	1.221	0.576	0.308	0.116
Mean OD	0.079	1.941	1.859	1.890	1.348	0.538	0.299	0.123
Mean OD-Mean Blank		1.8625	1.7800	1.8110	1.2695	0.4590	0.2200	0.0440
Standard deviation		0.0806	0.0049	0.0559	0.1796	0.0544	0.0134	0.0092
Standard error		0.0570	0.0035	0.0395	0.1270	0.0385	0.0095	0.0065
% Standard error		3.0604	0.1879	2.1208	6.8188	2.0671	0.5101	0.3490
% Viability		100	95.57	97.23	68.16	24.64	11.81	2.36

Table 8: Represents percentage cell viability of the control sample (without nanoparticles and resin nanocomposites, Sample 7) against NIH-3T3 fibroblast cell line.

			Concentration (in %v/v)					
	Blank	Untreated	1.25	2.5	5	10	20	30
Volume µL			2.5	5	10	20	40	60
Reading 1	0.08	1.998	1.683	1.852	0.765	0.458	0.16	0.118
Reading 2	0.077	1.884	1.678	1.866	0.787	0.404	0.244	0.083
Mean OD	0.079	1.941	1.681	1.859	0.776	0.431	0.202	0.101
Mean OD-Mean Blank		1.8625	1.6020	1.7805	0.6975	0.3525	0.1235	0.0220
Standard deviation		0.0806	0.0035	0.0099	0.0156	0.0382	0.0594	0.0247
Standard error		0.0570	0.0025	0.0070	0.0110	0.0270	0.0420	0.0175
% Standard error		3.0604	0.1342	0.3758	0.5906	1.4497	2.2550	0.9396
% Viability		100	86.01	95.60	37.45	18.93	6.63	1.18

5. Discussion

Green synthesis offers a sustainable approach with enhanced properties, significantly reducing environmental impact. The biosynthesis of ZnO NPs using plant extracts, bacteria, and fungi serves as a promising alternative to conventional chemical and physical synthesis methods. With the advancement of nanotechnology and its integration into dentistry, combining nanotechnology with nanocomposites presents a sustainable solution for oral health care. Restorative dentistry involves the filling of the oral cavity to inhibit the progression of secondary caries and prevent further deterioration. Incorporating ZnO NPs into resin-based nanocomposites offers a cost-effective and eco-friendly approach to develop materials with improved characteristics, potentially replacing conventional treatment materials. Restorative dentistry focuses on filling the oral cavity to halt the progression of secondary caries and prevent further deterioration. The incorporation of ZnO NPs into resin-based nanocomposites provides a cost-effective and environmentally friendly method for developing materials with enhanced properties. This approach has the potential to replace traditional treatment materials. One of the primary objectives of this study is to establish a streamlined method for fabricating resin nanocomposites.

In this study, we formulated ZnO NP-based resin nanocomposites by replacing the commonly used, yet expensive, resin monomer Bis-GMA with a blend of GMA and UDMA in a 60: 40 ratio. Mechanical testing indicated that the resin nanocomposites infused with ZnO NPs demonstrated enhanced tensile, flexural, and compressive strength at a concentration of 0.15 g ZnO NPs [11]. In contrast, TiO_2 NPs exhibited optimal performance at a lower concentration of 0.05 g. A similar trend was noted for flexural strength, where ZnO NPs showed improved performance at higher concentrations, whereas TiO_2 NPs performed better at lower concentrations [11]. Compression tests, including those conducted with commercial Dentsply Spectra samples, indicated that the highest compressive strength was achieved with 0.010 g of ZnO NPs and 0.15 g of TiO_2 NPs. The combination of ZnO and TiO_2 NPs at 0.1 g each demonstrated better compressive strength than the commercial Dentsply sample [11]. However, maximum compression was recorded for commercial ZnO powder, which may be attributed to nanoparticle agglomeration and structural inconsistencies as already reported [10].

Compared to commercial resin samples, ZnO NP-incorporated composites showed greater compression strain under moderate compressive forces, indicating enhanced flexibility, elasticity, and compatibility with the resin matrix likely due to surface modification. Conversely, commercial ZnO powders, consisting mostly of larger particles, demonstrated limited mechanical reinforcement due to poor dispersion, presence of impurities, and weak interfacial interaction with the resin [11]. At higher concentrations, both ZnO NPs and TiO_2 NPs exhibited increased compression strain, likely due to particle interference and disruption of resin-nanoparticle bonding, highlighting the need for precise optimization of nanoparticle incorporation.

Structural and functional group analyses were conducted on samples with the lowest concentrations selected based on mechanical performance results [11]. FTIR-ATR and FESEM techniques were employed to confirm the presence of functional groups and to analyse nanoparticle dispersion and interaction with the polymer matrix FTIR-ATR spectral analysis indicates the existence of functional groups at specific wavelengths, as illustrated in Figure 2, Figure 3 and Figure 4) for all three concentrations. Figure 2, Figure 3, and Figure 4 contain 0.05 g of ZnO NPs, 0.05 g of TiO_2 NPs, and

0.1 g of both ZnO and TiO_2 NPs, respectively, incorporated into resin nanocomposites. All three FTIR-ATR datasets were analysed comparably, and the functional groups were interpreted. Typically, all metals and metal oxides have reduced wave numbers below 1000 cm^{-1} as a result of interatomic vibrations [12], [13]. The range of 400-600 cm^{-1} corresponds to Zn-O vibrations, while 471-546 cm^{-1} denotes the stretching frequencies of Zn-O and Ti-O [12], [14]. The range of 800-900 cm^{-1} signifies the fingerprint region for ZnO NPs, TiO_2 NPs, the hydroxyl group of polyvinyl alcohol, and the presence of epoxy groups [13], [14].1034 cm^{-1} is the universal peak for all three samples, indicating the presence of C-O ester/ether groups inside the polymer matrix. The range of 1092-1094 cm^{-1} corresponds to the Si-O-C stretching vibration, mostly attributed to the utilization of APTES as a silane coupling agent [12]. The range of 1140-1142 cm^{-1} corresponds to the C=O stretching zone of esters, primarily attributed to methacrylate groups.1235 cm^{-1}, 1321 cm^{-1}, and 1373 cm^{-1} correspond to C-O, C-C, and C-N stretching vibrations associated with ester, amine, and carboxylate groups, respectively [12]. The range of 1401-1418 cm^{-1} signifies C-H and OH bending associated with COOH and alcohol, perhaps present on the surface of nanoparticles.1539-1576 cm^{-1} denotes the C=C and OH bending interactions between the resin matrix and nanoparticles.1634 cm^{-1} denotes the typical C=C stretching of methacrylate in conjugated dienes.1699-1705 cm^{-1} denotes the C=O stretching vibration for esters, acids, aldehydes, and ketones. A sharp peak (doublet) at 2350 cm^{-1}, primarily attributable to CO_2 entrapment [14].2933cm-2935 cm^{-1} signifies C-H stretching in alkanes, N-H stretching attributable to the polymer matrix of UDMA/GMA, and O-H stretching of alcohols. Consequently, FTIR data indicate the high purity of the synthesized ZnO NPs, TiO_2 NPs, and their amalgamation with the resin matrix.

Raman spectroscopy was utilized to clarify the molecular interactions and structural properties of dental resin nanocomposites containing ZnO NPs and TiO_2 NPs. The spectra, obtained over a 0 to 4000 cm^{-1} range with a 532 nm excitation laser, exhibited unique vibrational fingerprints characteristic of both the resin matrix and the embedded nanostructures. In Figure 5 (ZnO-resin composite), a significant band at 516.03 cm^{-1} corresponded to the E_2 (high) mode of the wurtzite phase of ZnO, hence validating the crystallinity of the nanoparticles [15], [16]. Supplementary peaks at 971.45 cm^{-1} (C–O–C stretching), 1854.61 cm^{-1}, and 2182.87 cm^{-1} indicated interactions between the polymer and nanoparticles, presumably due to overtones or second-order phonon scattering [17], [18]. Figure 6 (TiO_2 NPs based resin composite) exhibited distinctive peaks at 886 cm^{-1} (vibrations of ether or epoxide groups) and 1762 cm^{-1} (C=O stretching in ester linkages), thereby affirming the integrity of the methacrylate resin backbone. Significantly, peaks at 2121 cm^{-1} and 2182 cm^{-1} may signify alterations resulting from nanoparticle-matrix interactions or modified vibrational modes caused by TiO_2 dispersion [19], [20]. In the dual-nanoparticle system Figure 7, a medium-intensity band at 694 cm^{-1} may indicate the existence of rutile-phase TiO_2, while peaks at 969 cm^{-1} and 2182 cm^{-1} were ascribed to resin matrix vibrations and multi-phonon processes, respectively [21], [22]. The findings confirm the effective incorporation of ZnO and TiO_2 NPs into the resin matrix and underscore their potential to alter chemical bonding environments within the composite, potentially affecting the material's mechanical and antibacterial properties.

FESEM examination elucidates the surface morphology of the resin matrix incorporating nanoparticles, demonstrating the homogeneous dispersion or agglomeration of the particles, as illustrated in Figures 8, Figure 9, and Figure 10. The resin nanocomposites based on nanoparticles display comparatively smooth surfaces with localized aggregations of nanoparticles. The nanoparticles exhibit hexagonal or irregular morphologies, with scale bars of 10 µm and 3 µm utilized across all three samples. The discovered surface features, such as nanoparticle dispersion and shape, may enhance the antibacterial and antifungal capabilities of the composites. FESEM analysis revealed that ZnO NP-embedded samples displayed rod-shaped particles with dimensions below 100 nm, while TiO_2 NPs exhibited hexagonal or irregular morphologies ranging from 10 to 30 µm, often forming aggregates. Figure 9 (ZnO + TiO_2 NPs) showed better dispersion, suggesting improved biocompatibility and lower cytotoxicity. A rough surface with uniform dispersion generally indicated better integration, whereas roughness due to clustering suggested poor biocompatibility.

Table 2 to Table 8 represent the percentage of cell viability corresponding to increasing sample volumes from 2.5 µL to 60 µL showing a general trend of decreasing viability with increasing concentration. Table 2 demonstrates that the percentage viability decreases from 100% for untreated cells to 91.52% for 2.5 µL and 90.09% for 5 µL, indicating minimal cytotoxicity at lower doses. Upon further increase in volume, the viability drops to 57.83% at 10 µL and 46.82% at 20 µL. A sharp decline is observed beyond 20 µL, with viability reducing drastically to 1.50% and 1.48% for 40 µL and 60 µL, respectively. The calculated IC_{50} value is 6.37% v/v. A similar trend is observed in Table 3, where the percentage viability increases from 92.40% to 94.39% between 2.5 µL and 5 µL, followed by a significant drop to 1.26% at 60 µL, resulting in an IC_{50} of 7.13% v/v. In Table 4, viability increases from 92.32% to 99.09% and then decreases to 1.21%, also yielding an IC_{50} of 7.13% v/v. Table 5 shows a decrease in viability from 96.99% to 88.86% between 2.5 µL and 5 µL, continuing to drop to 1.91%, with an IC_{50} value of 6.32% v/v. Table 6 records a slight increase in viability from 96.32% to 98.20%, with an IC_{50} of 6.99% v/v. In Table 7, viability increases from 95.57% to 97.23% before falling to 2.36%, resulting in an IC_{50} of 6.74% v/v. Lastly, Table 8 shows an increase in viability from 86.01% to 95.60%, followed by a gradual reduction to 1.18% at 60 µL, with an IC_{50} value of 5.05% v/v.

In conclusion, ZnO NPs, when combined with the synthesized resin nanocomposites, demonstrate optimal cell viability at the lowest tested concentration (1.25% v/v), suggesting minimal cytotoxicity. The trend of increasing cell viability at low concentrations followed by a decline at higher volumes is especially evident in samples containing TiO_2 NPs with resin matrix, TiO_2 NPs and ZnO NPs together in resin matrix, ZnO NPs in commercial resin, ZnO powder in commercial resin, and the control samples. In contrast, a more consistent decrease in viability is observed for ZnO NPs in a synthesized

resin matrix and TiO_2 NPs in a commercial resin matrix. Therefore, across all samples (Table 2 to Table 8), the lowest concentration consistently supports higher cell viability, indicating that minimal concentrations are preferable for further biological applications.

6. Conclusion

Green-synthesized ZnO NPs are known to exhibit enhanced mechanical, physical, and chemical properties. Typically, Bis-GMA serves as a resin monomer; however, due to its high cost, this study has replaced it with glycidyl methacrylate (GMA) and urethane dimethacrylate (UDMA). Both GMA and UDMA are coated with APTES and PVA to create resin bio-nanocomposites. The composites exhibited enhanced tensile, compressive, and flexural strength at elevated concentrations of ZnO NPs, whereas TiO_2 NPs demonstrated similar performance at reduced concentrations as reported earlier [11].

The cytotoxicity study indicates that the combination of ZnO NPs with TiO_2 NPs resulted in improved outcomes, specifically higher cell viability and lower toxicity, compared to the control and other individual samples. Consequently, the other formulations may benefit from optimization by adjusting nanoparticle concentrations or modifying the nanocomposite synthesis procedure. These adjustments could lead to the development of more effective materials with tailored properties for specific applications. Further research will be essential to understand the mechanisms behind these interactions and to explore the potential of these optimized formulations in real-world scenarios.

This suggests that ZnO NPs, when used in combination with other nanoparticles, may offer superior cellular responses compared to individual nanoparticles, supporting their potential application in restorative dentistry. Further antibacterial studies are recommended using oral pathogens such as *Streptococcus mutans* and *Enterococcus faecalis* to determine the minimum inhibitory concentration (MIC) and identify the lowest effective dose for a concentration-dependent response. These investigations could provide valuable insights into the synergistic effects of these nanoparticles, ultimately leading to improved dental materials with enhanced antibacterial properties. Additionally, exploring the long-term stability and biocompatibility of these formulations will be crucial for their successful integration into clinical practice.

The formulations could also be investigated for wider applications across different areas of dentistry, such as periodontal and endodontic treatments. This exploration would further support a sustainable approach to addressing challenges related to dental and oral health. Additionally, research could be expanded to evaluate the long-term effects of these formulations on oral microbiomes and patient outcomes. By integrating these findings into clinical practices, dental professionals may enhance treatment efficacy while promoting overall oral health. Such advancements could lead to innovative strategies that not only improve patient care but also reduce the environmental impact of dental practices. As the field continues to evolve, collaboration between researchers and practitioners will be essential in translating these findings into real-world applications.

7. Future Scope

Future research will involve utilizing the composition of ZnO NPs-based resin nanocomposites to limit the proliferation of oral pathogens, specifically *S. mutans* and *E. faecalis*. Additionally, mechanical testing encompassing wear resistance, shock resistance, and biocompatibility assessment may be incorporated. The identical composition would also be applicable in several other areas of dentistry, including drug delivery systems, tissue regeneration, and root canal procedures. Cost-effectiveness is a significant element in promoting patient adoption of such products [23].

Conflict of Interest

The authors have no conflict of interest regarding this investigation.

Acknowledgement

The Authors would like to express sincere gratitude to the Cellkraft Biotech Pvt. Ltd, Bangalore for MTT assay studies. Special thanks to Dr. Heeresh Shetty of Nair Dental Hospital for his guidance and support.

References

[1] S. Malik and Y. Waheed, “Emerging applications of nanotechnology in Dentistry, ” *Dentistry Journal*, vol.11, no.11, p.266, 2023. doi: 10.3390/dj11110266.

[2] S. Malik, K. Muhammad, and Y. Waheed, “Emerging applications of nanotechnology in healthcare and medicine, ” *Molecules*, vol.28, no.18, p.6624, 2023. doi: 10.3390/molecules28186624.

[3] T. Barot, D. Rawtani, and P. Kulkarni, “Nanotechnology-based materials as emerging trends for dental applications, ” *Reviews on Advanced Materials Science*, vol.60, no.1, pp.173–189, 2021. doi: 10.1515/rams-2020-0052.

[4] M. Saridou, A. K. Nikolaidis, E. A. Koulaouzidou, and D. S. Achilias, “Synthesis and characterization of dental nanocomposite resins reinforced with dual organomodified silica/clay nanofiller systems, ” *Journal of Functional Biomaterials*, vol.14, no.8, p.405, 2023. doi: 10.3390/jfb14080405.

[5] G. Naguib, A. A. Maghrabi, A. I. Mira, H. A. Mously, M. Hajjaj, and M. T. Hamed, “Influence of inorganic nanoparticles on dental materials’ mechanical properties: A narrative review, ” *BMC Oral Health*, vol.23, no.1, 2023. doi: 10.1186/s12903-023-03652-1.

[6] Chaughule R, Raorane D, Pednekar S. Light curing dental nanocomposite resins using green synthesized TiO_2 nanoparticles as fillers. *Toxicology International*. [n. d.]. Available from: https: //www.tsijournals. com/abstract/light-curing-dental-nanocomposite-resins-using-green-synthesized-tio2-nanoparticles-as-fillers-14199. html

[7] R. Bourgi, Z. Doumandji, C. E. Cuevas-Suárez, T. B. Ammar, C. Laporte, N. Kharouf, and Y. Haikel, “Exploring the role of nanoparticles in dental materials: A comprehensive review, ” *Coatings*, vol.15, no.1, p.33, 2025. doi: 10.3390/coatings15010033.

[8] N. J., K. E., and R. S., "Green synthesis of zinc oxide nanoparticles: Eco-friendly advancements for biomedical marvels, " *Resources Chemicals and Materials*, vol.3, no.4, pp.294–316, 2024. doi: 10.1016/j. recm.2024.05.001.

[9] D. C. Bouttier-Figueroa, M. Cortez-Valadez, M. Flores-Acosta, and R. E. Robles-Zepeda, "Green synthesis of zinc oxide nanoparticles using plant extracts and their antimicrobial activity, " *BioNanoScience*, vol.14, no.3, pp.3385–3400, 2024. doi: 10.1007/s12668-024-01471-4.

[10] S. R. Wadekar, M. S. Hate, and R. Chaughule, "Biosynthesis of zinc oxide nanoparticles and their cytotoxicity study on fibroblast cell line using MTT assay, " *Oriental Journal of Chemistry*, vol.41, no.2, 2025. [Online]. Available: https: //www.orientjchem. org/vol41no2/biosynthesis-of-zinc-oxide-nanoparticles-and-their-cytotoxicity-study-on-fibroblast-cell-line-using-mtt-assay/

[11] S. R. Wadekar, M. S. Hate, and R. Chaughule, "Biosynthesis of ZnO NPs-Based Resin Nanocomposites: A sustainable oral health care solution, " *Oriental Journal of Chemistry*, in press, 2025.

[12] H. Team, "FTIR Functional Group Database Table with Search-InstaNANO, " *InstaNANO*, Mar.28, 2023. [Online]. Available: https: //instanano. com/all/characterization/ftir/ftir-functional-group-search/

[13] N. Annu, Z. I. Bhat, K. Imtiyaz, M. M. A. Rizvi, S. Ikram, and D. K. Shin, "Comparative study of ZnO-and-TiO2-nanoparticles-functionalized polyvinyl alcohol/chitosan bionanocomposites for multifunctional biomedical applications, " *Polymers*, vol.15, no.16, p.3477, 2023. doi: 10.3390/polym15163477.

[14] Y. Xia, F. Zhang, H. Xie, and N. Gu, "Nanoparticle-reinforced resin-based dental composites, " *Journal of Dentistry*, vol.36, no.6, pp.450–455, 2008. doi: 10.1016/j. jdent.2008.03.001.

[15] I. Saleem, N. F. Rana, T. Tanweer, W. Arif, I. Shafique, A. S. Alotaibi, H. A. Almukhlifi, S. A. Alshareef, and F. Menaa, "Effectiveness of SE/ZnO NPs in enhancing the antibacterial activity of resin-based dental composites, " *Materials*, vol.15, no.21, p.7827, 2022. doi: 10.3390/ma15217827.

[16] Raman Band Correlation Table, 2021. [Online]. Available: https: //www.chem. uci. edu/~dmitryf/manuals/Raman%20correlations. pdf

[17] C. Klingshirn, "ZnO: From basics towards applications, " *Physica Status Solidi (B),* vol.244, no.9, pp.3027–3073, 2007. doi: 10.1002/pssb.200743072.

[18] M. Gaintantzopoulou, S. Zinelis, N. Silikas, and G. Eliades, "Micro-Raman spectroscopic analysis of TiO2 phases on the root surfaces of commercial dental implants, " *Dental Materials*, vol.30, no.8, pp.861–867, 2014. doi: 10.1016/j. dental.2014.05.030.

[19] D. Bersani, P. P. Lottici, and A. Montenero, "Micro-Raman investigation of iron oxide films and powders produced by sol–gel syntheses, " *Journal of Raman Spectroscopy*, vol.30, no.5, pp.355–360, 1999. doi: 10.1002/ (SICI) 1097-4555 (199905) 30: 5<355:: AID-JRS398>3.0. CO; 2-C.

[20] N. T. Huey, T. M. Greve, S. Kamp, and G. B. E. Jemec, "Disease quantification in dermatology: In vivo near infrared spectroscopy measures correlate strongly with the clinical assessment of psoriasis severity, " *Journal of Biomedical Optics*, vol.18, no.3, p.037006, 2013.

[21] T. Ohsaka, "Temperature dependence of the Raman spectrum in anatase TiO2, " *Journal of the Physical Society of Japan*, vol.48, no.5, pp.1661–1668, 1980. doi: 10.1143/jpsj.48.1661.

[22] O. Frank, M. Zukalova, B. Laskova, J. Kürti, J. Koltai, and L. Kavan, "Raman spectra of titanium dioxide (anatase, rutile) with identified oxygen isotopes (16, 17, 18), " *Physical Chemistry Chemical Physics*, vol.14, no.42, p.14567, 2012. doi: 10.1039/c2cp42763j.

[23] Narang J. Narang R. Nanomedicines for dental applications—scope and future perspective. International Journal of Pharmaceutical Investigation.2015; 5 (3): 121. doi. org/10.4103/2230-973x.160843.

Author Profile

Ms. Shravani R. Wadekar is currently pursuing a Ph. D. from Ramnarain Ruia Autonomous College under the guidance of Prof. Dr. Manish Hate and Prof. Dr. Ramesh Chaughule. Her research focuses on nanotechnology and its diverse applications in food packaging, wound healing, agriculture, and dentistry. She has developed eco-friendly bio-nanocomposite films as sustainable alternatives to conventional plastics, aiming to enhance shelf life and reduce environmental impact of food products which is usually caused by plastic pollution". Her work has been recognized with prestigious accolades, including a Gold Medal at the 17 th Maharashtra State Level "AAVISHKAR" Research Convention 2025 and Silver Medal at West Zone Student Research Convention "ANVESHAN" 2025. Also, have been selected to represent Mumbai University at the International Research Convention 2025. Additionally, She hsd published three research papers entitled with "Development of Eco-friendly bio-nanocomposites films for prolonging shelf-life in food packaging", "Increasing shelf life of millets by developing bio-nanocomposite films (bioplastic) as an alternative to conventional plastic", "Biosynthesis of Zinc Oxide Nanoparticles and its evaluation for MTT Cytotoxicity and Wound Healing Using NIH-3T3 Fibroblast Cell Line", and "Biosynthesis of Zinc Oxide Nanoparticles and Their Evaluation for Wound Healing Application Using NIH-3T3 Fibroblast Cell Line", along with eleven book chapters based on various application. Through her research, she aims to bridge the gap between scientific innovation and real-world applications by developing sustainable, high-performance materials that contribute to environmental conservation, improved healthcare solutions, and advancements in agricultural and food packaging technologies.